Finite Difference Time Domain (FDTD) Characterization of a Single Mode Applicator

S. K. Pathak, F. Liu and J. Tang

Microwave heating plays an important role in the processing & heating of foods in the food industry and at home, but the applicator design is frequently an arduous task. The finite-difference time-domain (FDTD) method can be used to model complex geometries and guide the design of different types of applicators. In the reported research, the FDTD approach has been employed to characterize the electric field distribution of a rectangular waveguide applicator, carrying TE_{10}-mode aperture field distribution, terminated in an oversize rectangular waveguide/ cavity and operating at 915 MHz. A comprehensive study was carried out to evaluate the mode/field distribution in the empty cavity box as a function of its geometrical dimensions. Power deposition profile throughout the volume of a packaged food, and scattering parameters as a function of food properties and surrounding environment were computed, by using a realistic food-engineering model. Good agreements between modeling and experimental results were obtained. The results demonstrated the usefulness of numerical simulation in predicting and characterizing the electromagnetic (EM) field distributions in microwave applicators used in food processing.

Keywords: Microwave Heating, Waveguide, Cavity, Mode Distribution, Power Deposition distribution, S-parameter, Finite Domain Time Domain (FDTD) method

S. K. Pathak is at the Institute for Plasma Research, Bhat, Gandhinagar, India. F. Liu and J. Tang are affiliated with Biological System Engineering at Washington State University in Pullman, Washington, USA.

One of the crucial technical challenges facing engineers and scientists working in the area of microwave heating is the ability to predict heating patterns and to control the amount of energy that is deposited within the heated region. This ability is desirable in the design and operation of food processing systems based on microwave energy. However, predicting the heating pattern and the energy deposited within a foodstuff from microwave heating applicators has proven to be a difficult task due to the complex nature of the interaction mechanism and governing physics [Metaxas and Meredith, 1983; Metaxas, 1996; Roussy and Pearce, 1995; Decareau, 1985]. The large variety of materials and foods, their property compositions, geometric configuration, and processing requirements make the analysis and modeling even more complicated.

Several different numerical schemes have been used to predict electromagnetic fields in microwave heating. Dibben and Metaxas [1997] used the finite element time domain method (FETD) and concluded that time domain simulations of microwave heating problems overcome the problems of ill-conditioning and are much more rapid than frequency domain method. The time domain method is also advantageous when solutions at a range of frequencies are required since Gaussian pulse excitation allows several results to be extracted from a single solution. Explicit integration of Maxwell's equations in space and time eliminates the need for storage and inversion of large matrices, which is unavoidable in finite element method (FEM). The present study focused on computational modeling of microwave heating applicator by using the universal Electromagnetic simulator *QuickWave-3D*, implementing the conformal Finite Difference

Time Domain Method (FDTD) [Mirotznik, 1998; Celuch and Gwarek, 2000; Marcysiak and Gwarek, 1994; Marcysiak, 1996; Marcysiak et. al, 1998, and Marcysiak and Gwarek, 1999]. The method implemented in *QuickWave-3D* goes further: it works efficiently with large and small permittivities of the heated materials and places modest requirements on computer memory. The main advantage of conformal *QuickWave-3D* version compared to the classical FDTD method, pioneered by Yee [1966], is the flexibility of the shape of individual cells used to discretize the simulated domain. This removes the limitation of the classical FDTD: the necessity of staircase approximation of curved boundaries. Successful applications of *QuickWave-3D* in microwave heating problem are reported in the literature [Risman, 1998]. The salient features of the software are [Celuch and Gwarek, 2000]:

a) it provides accurate and stable representation of curved metal boundaries;
b) it provides higher order modeling of media interfaces and allows wide-band modeling of skin effect in lossy metals;
c) it provides spurious-free behavior of the algorithm, also in the presence of strong spatial irregularities;
d) the software allows matched modal excitation based on the field and impedance template; and
e) the software uses a novel variable source impedance technique for emulation of pure eigen-modes in inhomogeneous resonators, among other things.

A simple yet frequently used microwave applicator for heating in industries and microwave oven is a simple straight fundamental mode waveguide. An open-ended direct contact waveguide type of microwave applicator has been characterized from theoretical and experimental perspectives in past in non-food applications [Guy et. al., 1978; Guy, 1971; Turner and Kumar, 1982; Lau et. al., 1986; Kantoor and Cetas, 1977; Kantoor, 1981; Waterman and Nerlinger, 1986]. Guy [1978 and 1971] developed mathematical expressions based on Fourier transforms of the aperture field to predict the heating patterns of a rectangular waveguide in bilayered tissue models of muscle and fat. He studied the effects of aperture dimensions and frequency on the depth of penetration and on overall distribution of heating patterns. The theoretical results were compared with experimental data with good agreement. Turner and Kumar [1982], by using Huygens' equivalence principle of aperture current, numerically solved the EM field distribution in a homogeneous dielectric medium. In their simulation, a waveguide was uniformly loaded with a dielectric medium, but influence of the applicator dimensions in shaping the fields within the irradiated region was not included. Further, these theoretical methods were limited to the media with infinite extent in the region in front of the applicator.

The FDTD method has been applied in a three-dimensional numerical model of a circular waveguide applicator with a dielectric lens of deionized water irradiating tissues at 433 MHz [Lau et. al., 1986]. An experimental arrangement to measure the electric field components in the phantom was used. Again, excellent agreement was found in comparisons between theory and experiments. Lau [1986] found that FDTD simulation accurately predicted EM-field distribution of the applicator. However, the applicator was designed to provide focused and localized field distribution.

The thermographic technique demonstrated by Guy [1978] has been extensively used for empirical characterizations and for evaluating the heating patterns of various types of microwave (MW) applicators when irradiating tissue-equivalent phantoms [Kantoor and Cetas, 1977; Kantoor, 1981]. Waterman and Nerlinger [1986] measured Specific Absorption Rate (SAR) distributions associated with a rectangular slab-loaded waveguide when coupled to a phantom via materials of different dielectric constants. Their work demonstrated

that the coupling material had a marked effect on the SAR distribution. Although no attempt was made to explain these results theoretically, the results indicate a need for a basic understanding of the behavior of EM fields in the vicinity of MW applicators and coupling media such as those routinely countered.

The objectives of this research were to study the modal and near field characterization of a waveguide (WR975) terminated in the oversized rectangular waveguide/ cavity. The frequency of 915 MHz was chosen in the present study because microwaves at this frequency provide deeper penetration depth as well as better/larger delimitation of the volume of heating materials compared to 2450 MHz. The studies were divided into two parts. In the first part, the aperture field distributions in the smaller waveguide and electric field distribution (dominant electric field component) at any point in the cavity box were computed as a function of geometrical dimensions of the rectangular cavity box.

In the second part, the realistic use of the applicator in possible food processing applications was assessed. Here, near field power deposition profiles throughout the food package volume and scattering matrix, which explains power coupling aspects, were studied with respect to geometrical parameters of the cavity and the electrical properties of the food materials/packages. Experiments were conducted to validate the findings of the proposed model.

Design and Characteristics of Microwave Applicators

General Characteristics

Usually, the design of microwave applicator, which couples the microwave energy to the load, follows one of the following four fundamental principles:

- **Single-mode cavities:** These are designed to operate with only one, or a few, resonant modes in small well-defined volume [Metaxas and Meredith, 1983; Metaxas, 1996; Roussy and Pearce, 1995; Decareau, 1985].
- **Multimode cavities:** These are designed for large volumes (relative to wavelength) where the heating patterns/distributions are determined by interaction of large number of cavity modes [Metaxas and Meredith, 1983; Metaxas, 1996; Roussy and Pearce, 1995; Decareau, 1985].
- **Radiation applicators:** These are designed on the basic principle of microwave antennas radiation in which outgoing/propagating microwave energy propagates freely in the load like free space wave, without being substantially bounded to the certain geometry [Metaxas and Meredith, 1983; Metaxas, 1996; Roussy and Pearce, 1995; Decareau, 1985].
- **Traveling wave applicators:** These are designed on the basic principle of guided mode propagation in which microwave energy is confined in the well-defined geometry. The power fed into these applicators are substantially absorbed by a well-matched workload in it during one pass of the wave, with residue being dissipated in an absorbing terminal load.

Our studies focused on single-mode cavities, because of the possibility to gain a knowledge of well-defined EM field distributions, which enables the food material under treatment to be placed in the position of maximum & uniform electric field for optimal transfer of microwave energy.

Computer Simulation of the Present Model

Model and simulation procedure

Figure 1(a) represents a fundamental mode in a rectangular waveguide, and Figure 1(b) depicts a conceived model used in this study. It is visualized by the Editor in 3D of Quick-Wave software, where a WR975 waveguide is termi-

a)

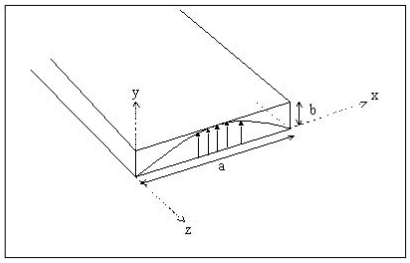

b)

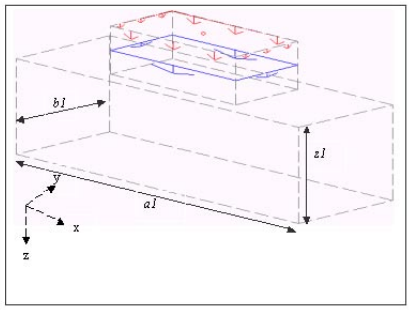

Figure 1: *a) Geometrical configuration/representation of a fundamental mode (TE_{10}-mode) in a waveguide (a = 248 mm and b = 124 mm) and b) Two rectangular waveguides coupled to each other. The second waveguide is an oversized rectangular waveguide/cavity.*

nated into an oversized rectangular waveguide/ cavity. The dimensions of standard WR-975 waveguide are a = 248 mm and b = 124 mm for 915 MHz systems. For this waveguide, the lowest order-propagating mode will be TE_{10} (m = 1, n = 0), which is also called the dominant mode of the rectangular waveguide. Aside from the degree of match between exciting waveguide and the oversized waveguide itself, all the properties of interest relate to the aperture field from the open end of the main waveguide.

In the computer model, excitation of the device is assigned through the port (Figure 1(b)) simulating the presence of dominant TE_{10}-mode in the input waveguide cross-section. The model was discretized with the standard FDTD "rule of thumb" suggesting the use of at least ten cells per wavelength in the medium with permittivity ε:

$$\Delta cell \leq \frac{c}{10 f \sqrt{\varepsilon}}, \qquad (1)$$

where c is velocity of light (m/s), f is frequency (Hz) and ε is the permittivity values of the medium. Therefore, free space cell size should be less than 33 mm in all x-, y-, and z- directions at 915 MHz. For the present model, Figure 1b, cell sizes were 10 mm in all three dimensions. The simulations were run on a Pentium Personal Computer with an 850 MHz processor and 256 MB RAM under a Windows NT 4.0 operating system.

Modal Characteristics

From knowledge of the transverse electromagnetic field at the aperture of a coupling waveguide, it is possible to predict various characteristics of the oversized cavity box. One such characteristic is dominant electric field distribution (in present study E_y– component) throughout the space in the cavity box. The mode distributions were simulated as a function of x-, y- and z –dimensions of the cavity. The x-dimension, *a1*, was changed from *1.0*a* to *2.5*a*, the y-dimension, *b1*, was changed from *1.0*b* to *2.0*b* and the z-dimension, *z1*, was changed from 100 to 200 mm, respectively. Main findings from theses simulations are discussed below. These characteristics were aimed to determine the mode distribution (other than TE_{10}-mode) inside the oversize waveguide/ cavity with its changing dimensions. The information will include how and where the microwave energy is distributed inside the cavity which, in turn, will help us decide where and what size of the food package should be placed inside the cavity to provide relatively uniform heating.

Effect of Change in X-Dimension of the Cavity on the Mode Distribution

Figure 2 gives a detailed mode distribution characteristic in the terminating cavity box as a function of the cavity dimension, *a1*, (along the x-axis in Figure 1). The narrower dimension, *b1*, (along the y-axis in Figure 1) of the cavity was same as the WR975 waveguide dimension. As we know that the depth of penetration in high

loss food material is very small (depends upon the food permittivity-values), therefore, the depth of the cavity, *z1*, was restricted up to 200 mm in our studies. Figures 2(a,b,c) show the dominant electric field component (E_y, which was more than eight times stronger than other electric field components, E_x & E_z) distribution over xy-plane for the various dimension of *a1* at the middle layer of the cavity box (*z1* = 100 mm). From the distribution it is clear that for small *a1* values, energy was distributed mainly around the center of the xy-plane in a single mode. As *a1* increased, the spread area of single mode energy increased, but after certain value of *a1*($\geq 2.0 * a$) the electric field was split into two modes in x-direction. Therefore, for single mode confinement in the cavity box the x-dimension of the cavity can not be more than two times the WR-975 waveguide dimension in the present example model. This observation was more pronounced in the xz-plane distribution, which is shown in the Figures 2(d,e,f). This type of cavity field distribution, as observed in Figures 2(b) and 2(e), is suitable for the case where relatively large and flat profile (~250 mm x 120 mm x 30 mm, in x-, y- and z- direction, respectively) food stuff (e.g., pizza, or shallow food trays) need to be heated.

Effect of Change in y-Dimension of the Cavity on the Mode Distribution

Figure 3 explains the modal distribution characteristics across the cavity as the narrow side dimension changed. In the present scenario, x-dimension, *a1* (larger dimension of cavity), of the cavity box was set equal to the larger dimension, *a*, of WR-975 waveguide and cavity depth, *z1*, was 200 mm, as in the previous case. As the narrow side of the cavity box, *b1*, increased, the energy was more focused as a pencil beam at the center point of the cavity in xy-plane, as shown in the Figures 3 (a,b,c). This characteristic was more clearly visible in the yz-plane characteristics, as shown in Figures 3 (d,e,f). This characteristic of waveguide has been fully exploited in Antenna Engineering, where focused beam of microwave energy is needed to guide the energy. The foodstuffs, which have smaller cross-section and larger lateral/axial depth, will find this type of applicator more suitable, where focused microwave energy is needed for heating.

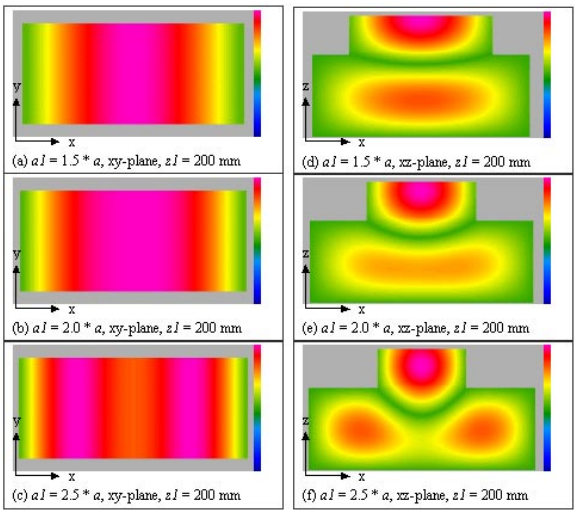

Figure 2: *The dominant electric field (E_y-component) distribution across xy- plane (at middle of z1) and xz-plane (at middle of b1) of the cavity box (b1=b) as a function of larger (x-dimension) dimension, a1.*

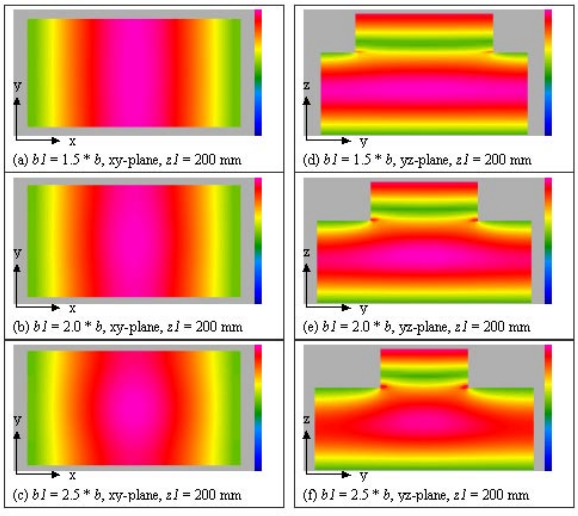

Figure 3: *The dominant electric field (E_y-component) distribution across xy- (at middle of z1) and yz-plane (at middle of a1) of the cavity box (a1=a) as a function of narrower (y-dimension) dimension, b1.*

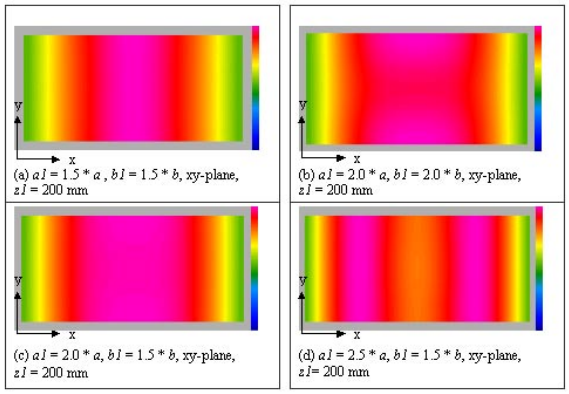

Figure 4: *The dominant electric field (E_y-component) distribution across xy-plane (at middle of z1) of cavity box as a function of x- and y- dimensions of the cavity box.*

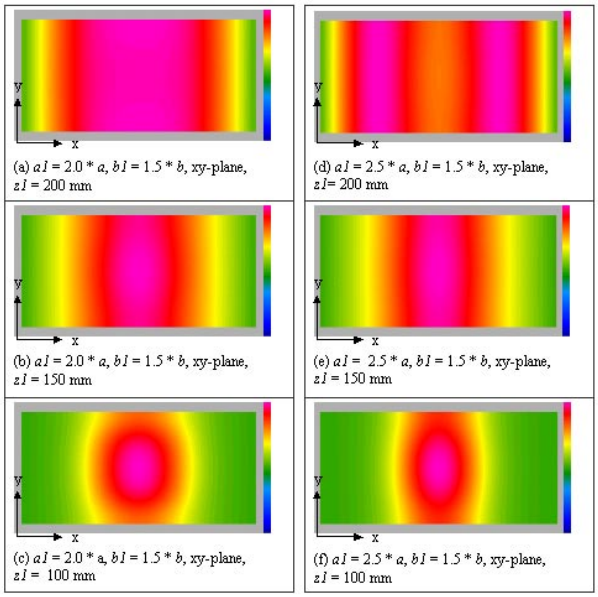

Figure 5: *The dominant electric field (E_y-component) distribution across xy-plane (at middle of z1) of cavity box as a function of x-, y- and z- dimensions of the cavity box.*

Effect of Change in Both x- and y-Dimensions of the Cavity on the Mode Distribution

Figure 4 shows the combined effect of changing x- and y- dimensions of the cavity on the mode distribution across xy-plane. It is clear that for a single mode confinement in the cavity box we have to choose both x- and y-dimension very carefully. As shown in Figure1(a), the polarization of electric field was along y-axis and it was distributed as a half sine wave over the aperture of waveguide along x-axis. As x-dimension of the cavity box increased while keeping y-dimension unchanged, the half sine wave distribution of the wave entering the cavity from fundamental waveguide mouth was stretched along x-axis and resulted in a spread of energy distribution, as in case of TE_{10}-mode distribution of Figures 2(a-f) and Figure4c. On the other hand when y-dimension of the cavity was increased, while keeping x-dimension same as WR975 waveguide dimension, *a*, there was more concentration of electric filed lines towards the center of the cavity. This led to a focused energy distribution, as shown in Figures 3(a-f) and Figure 4(a).

The effect of changing both the dimension of the cavity is shown in Figure 4. Wavefront emanating from the waveguide aperture experienced a radial spread in wavefront and introduced a phase component between the wavefronts at different axial locations of the cavity. When this phase component became large enough between WR975 waveguide aperture and variable axial location aperture inside the cavity, the field distribution in the cavity was split into two directions and its reflection from respective direction cavity wall formed two modes, as shown in Figures 4(b) and 4(d). In Figure 4(b), a change in *b1*-dimension was responsible for the phase component in wavefronts, while in Figure 4(d) changes in *a1*-dimesnion were responsible for the phase component.

Effect of change in z-dimensions of the cavity on the mode distribution

Figure 5 shows the effect of cavity depth variation on mode distribution over xy-plane of the two cavities having dimensions: *a1 = 2.0*a & b1 = 1.5*b* and *a1 = 2.5*a & b1 = 1.5*b*. As

cavity depth was increased, the wave emanating from the waveguide traveled more distance in the cavity space, which introduced large phase component between the two wavefronts, resulting in the split of field distribution, as is evident from Figure 5(d). But for a smaller cavity depth, due to very small changes in phase components, the field distribution was mainly centered around the central region, as seen in Figure 5(b,c,e,f), of the cavity box. Therefore, a very small area of the cavity box is available for placing the foodstuff with relatively uniform power depositions.

In conclusion, choosing proper x-, y- and z-dimensions of the cavity box, we can use this type of applicator as a single mode cavity to provide a well-defined field distribution with a higher power density. In the present model configuration the upper limits for *a1*, *b1*, and *z1* are respectively equal to 2**a*, *1.5*b*, and 200 mm. The corresponding field distribution is shown in Figure 5(a).

Evaluation of the Applicator with a Realistic Food-Engineering Model

The previous section has shown the effect of geometrical dimensions of the applicator on mode behaviors when wave propagates/radiates in an empty cavity. The performance of the applicator was then considered with a realistic model consisting of a food package kept in the near field/aperture field of the waveguide, as shown in Figure 6. Two fixed-cavity box dimensions: *a1* = 2.0**a*, *b1* = 1.5**b*, and depth of cavity *z1* = 100 mm & 150 mm, respectively, were chosen for the present model. The food dimensions were 140 x 100 x 30 mm and the value of complex permittivity, $\varepsilon^* = \varepsilon' - j\,\varepsilon''$, of food (whey gel as a model food) was 47.45 – j 38.55 at 915 MHz at room temperature.

Modeled Power Deposition Pattern

As the energy propagates, the food package absorbs a substantial amount of energy from the exponentially decaying microwave power in accordance with the dielectric properties of the food. The power deposition profile over top surface of the food package was calculated in two different situations. In the first case, the food package was kept in the central region of the cavity in open air. In the second case, the food package was immersed in water (complex permittivity, $\varepsilon^* = 71.21 - j\,16.76$). Following the criterion of equation (1), the cell size in air space region of the waveguide was chosen to be 10 mm in x- y- and z-directions. Food and water cell size dimensions were 8 mm in the x- & y- direction and 3 mm in the z- direction, respectively.

Figure 7 shows the power deposition pat-

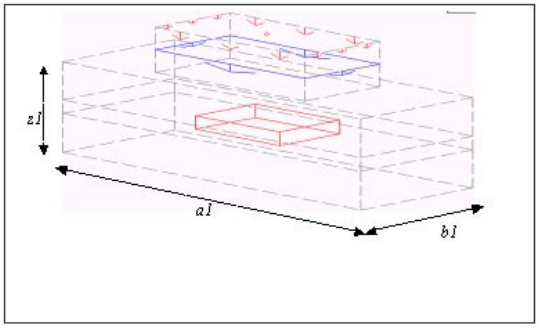

Figure 6: *A rectangular waveguide is terminated with a rectangular cavity loaded with a gel slab (140X 100X 30 mm)*

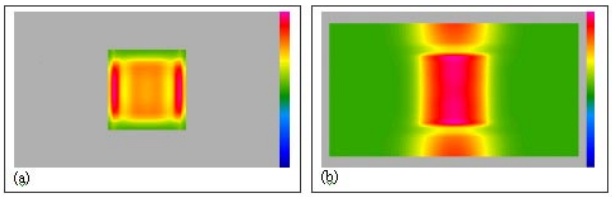

Figure 7: *a) Computed power deposition profile over top surface (xy-plane) of a gel slab (in open air). Cavity dimensions: a1 = 2.0*a, b1 = 1.5 *b, and z1 = 100 mm and gel slab dimensions = 140x100x30 mm. b) Computed power deposition profile over top surface (xy-plane) of a gel slab (immersed in water). Cavity dimensions: a1 = 2.0*a, b1 = 1.5 *b, and z1 = 100 mm and gel slab dimesion = 140x100x30 mm.*

tern over the food package in the two different situations. When a food package was heated in air within the cavity, the power deposition at the edges was much higher than that in the middle region, resulting in a very uneven power deposition pattern. Also, it is observed that electric field in the food package was split into two different high power zones in spite of the fact that only a single mode was generated in the empty cavity of the same dimension (see Figure 5(c)). This might have been the result of reflection and refraction of the waves at the interfaces between the food package and the surrounding air, as well as the discontinuity of the electric- and magnetic- field components at the food-air interfaces. When microwave energy was incident on the food package, the electric field distribution of the incident mode was responsible for the power deposition pattern. Slight deviations in electric field distribution cause large deviations in power deposition patterns. In Figure 7(b), when food package was immersed in water having dielectric property that better matched (than air) with that of food, the power deposition profile over the food package was in single lobe and uniform, compared to the earlier cases. This improved the uniformity of absorbed power distribution in the food package. Because water acted as a matching medium, the energy from the microwaves was easily transmitted directly to the bulk of food package. In this case it is seen that the concentration of the electric field at the center was greater than at the x-side edges. But there was slightly more power deposition at the y-side edges due to the fact that electric field lines were along the y-axis and concentration of the field at the tip of sinusoidal distribution was more in comparison to the sides.

Experimental Procedure and Verification of Simulation Results

Experimental Procedure

To verify the simulation findings, sets of experiments were performed with an applicator cavity made of aluminum plates with dimensions as mentioned in section 2.2. A 20 kW 915 MHz microwave power source manufactured by Ferrite Company, Inc. (FCI, Hudson, NH) was used for coupling the microwave power in the cavity through a WR975 waveguide. The reflection of the power was measured with a built-in directional coupler in the source and a HP power meter (436A). A moderate power level of 6 kW was delivered to the load to obtain reasonable heating time (0.5 to 2 minutes) to allow 30^0C to 64^0C rise in the food temperature and yet to minimize the influence of heat conduction. The microwave power distribution pattern dissipated in/over the food load surface was indirectly measured by temperature via an infrared camera (model Thermal CAM™ SC-3000, N. Billerica, MA). The ThermaCAM SC-3000 QWIP sensor provided an image resolution of 320 x 240 pixels, captured real-time dynamic events using the camera's digital output at 5 images per second. This camera analyzed individual frames that cover a wide temperature range (-40 to 120°C), and provided resolution of 0.1°C. The thermal imaging gave an accuracy of ±2% of the measured temperature range (20-70°C in our studies).

Verification of Field/Mode Distribution in an Empty Cavity

To verify the field distribution characteristics, y-polarized dominant electric field component (E_y-component) strength, which was over eight times stronger than other electric field components, throughout the cavity space was to be measured. This was a very tedious task because it was almost impossible to insert an array of microwave electric field detecting probes to measure the field pattern inside the cavity. To simplify this measurement, a thin wet paper was placed in the middle xy-plane of the cavity (having dimensions: $a1 = 2.0*a$, $b1 = 1.5*b$, and depth of cavity $z1$ = 100 mm & 150 mm, respectively) as an indirect way to measure the intensity of electric field pattern in an empty cavity. Microwave

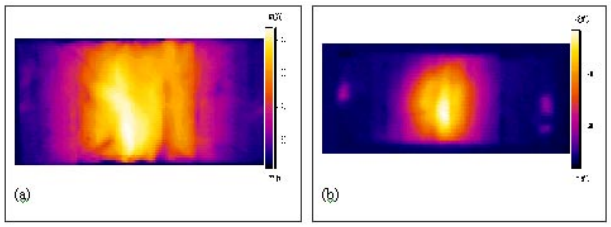

Figure 8: *a) Experimental temperature distribution over top surface (xy-plane) of the wet paper spread in the middle cross section of the cavity (cavity dimensions: a1 = 2.0*a, b1 = 1.5 *b, and z1 = 150 mm) b) Experimental temperature distribution over top surface (xy-plane) of the wet paper spread in the middle cross section of the cavity (cavity dimensions: a1 = 2.0*a, b1 = 1.5 *b, and z1 = 100 mm)*

power was delivered to the cavity for 0.5 min, and the paper was immediately taken out from the cavity for infrared imaging. The images are shown in Figure 8 for two cavity depths 150 mm & 100 mm, respectively. These patterns compare well with simulated patterns of electric field (E_y-component) intensity as shown in Figures 5(b) and 5(c), respectively, for the respective cavity depths. Although the patterns shown in Figure 8 reflects absorbed power distribution patterns, not the field distribution, but this clearly verified our earlier simulation that only one mode of distribution was present in the unloaded cavity. From the images it can be seen that electric field was concentrated in the center of the cavity and its intensity decreased towards x-direction from the center of the cavity box.

Verification of Power Deposition Pattern in Loaded Cavity

To find the absorbed power deposition pattern for a real food-engineering model, a whey gel protein was used as a model food. The dielectric properties of the material used in computer simulation were determined in a custom-built temperature-controlled test cell and with an Agilent 4291 impedance analyzer. Details of the dielectric property measurement system and procedures are described in Wang et. al. [2003].

The model food was heated in a 915 MHz cavity. The cavity dimensions were *a1* = 2.0**a*, *b1* = 1.5 **b*, and *z1* = 100 mm. Experimental power deposition characteristics on whey gel slab (140 x 100x 30 mm) without water and with water, are shown in Figures 9a & 9b, respectively. From Figures 7a and 9a, without water around the food package, both simulated and experimental patterns were similar. However, when the food package was immersed in water, a slight deviation in power deposition patterns was seen (Figures 7(b) and 9(b)). As observed

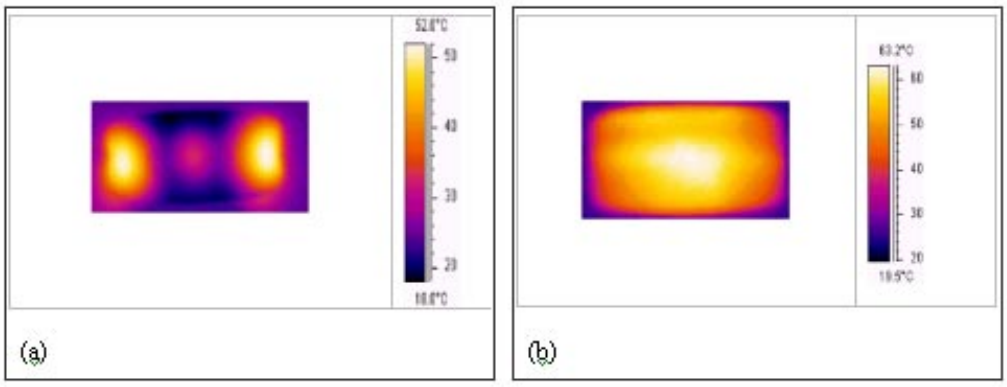

Figure 9: *a) Experimental temperature distribution over top surface (xy-plane) of a food gel slab package (in open air). Cavity dimensions: a1 = 2.0*a, b1 = 1.5 *b, and z1 = 100 mm and gel slab dimensions = 140x100x30mm. Images are shown only on gel slab surface. Cavity space is not shown. b) Experimental temperature distribution over top surface (xy-plane) of the food package (immersed in water). Cavity dimensions: a1 = 2.0*a, b1 = 1.5 *b, and z1 = 100 mm and gel slab dimensions = 140x 100x 30mm. Images are shown only on gel slab surface. Cavity space is not shown.*

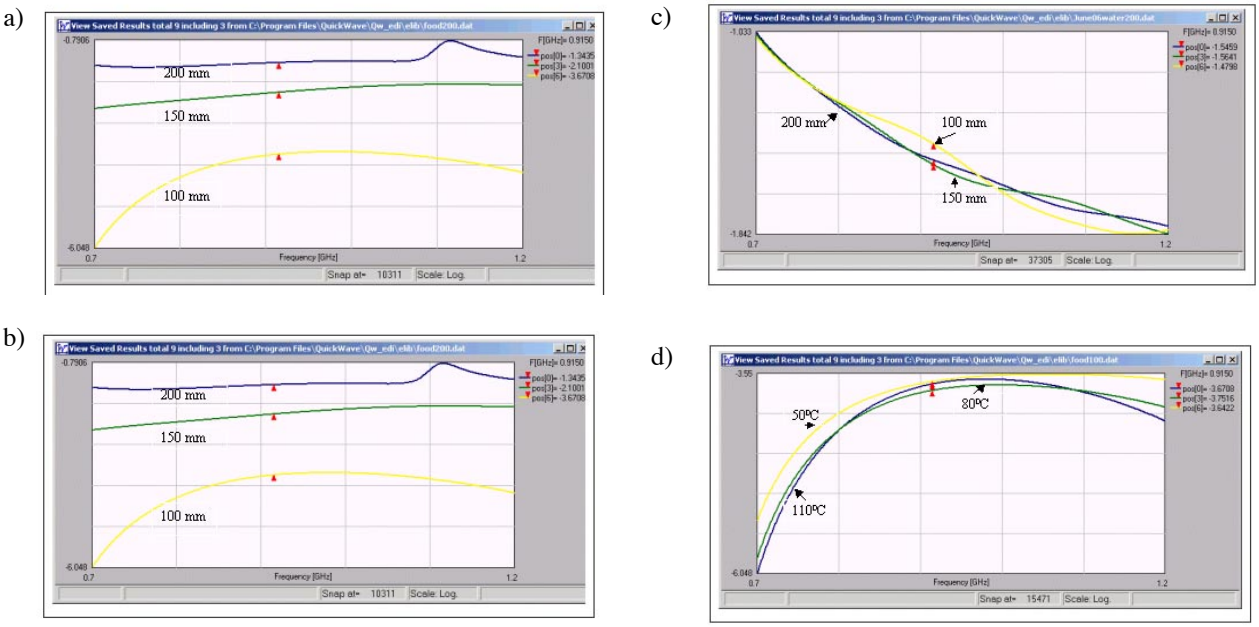

Figure 10: *Computed return loss (S_{11}-parameter, in dB): a) in the frequency spectrum 0.7 to 1.2 GHz lying around 915 MHz as a function of cavity box depth (empty cavity); b) in the frequency spectrum 0.7 to 1.2 GHz lying around 915 MHz for the cavity with a food tray; c) in the frequency spectrum 0.7 to 1.2 GHz lying around 915 MHz as a function of cavity box depth. A food tray, immersed in water, is placed in the cavity; and d) in the frequency spectrum 0.7 to 1.2 GHz lying around 915 MHz as a function of food temperature. A food tray is placed in the cavity.*

in both cases, the hot zone in the food packages was at the center of the surface of load and its density decreased along the x-direction of the model food package load. However, overheating at the edges, in experimental findings, in y-direction was not visible as in the simulated results. In simulation, by varying the height of the load and load position in x- and y-directions ± 10 mm, a series of simulations was performed, but some overheated patterns at the edges in the y–direction were always observed. This slight disagreement between model prediction and experimental findings might have been due to some heat conduction as well as some radiation loss during the transit between cavity location and infrared camera location, that was not taken into account in the modeling results.

Scattering Matrix/Matching

The S-parameter, S_{11}, which explains return loss and efficiency of the applicator, was computed in the frequency spectrum 700 – 1200 MHz (0.7 – 1.2 GHz). The parameter was computed in three different situations: empty cavity box, with food package without water and food package immersed within water. Cavity dimensions are $a1 = 2.0*a$, $b1 = 1.5 *b$, and various $z1$-values. Figure10(a) captured directly from the QuickWave-3D simulator shows the return loss behavior of the empty cavity box within frequency spectrum 700 to 1200 MHz at different cavity depths. The resonant mode was in the high frequency end of the spectrum. As cavity depth increased, the resonant frequency gradually shifted to the lower frequency spectrum. Figure 10(b) explains the return loss behavior within the frequency spectrum with different cavity depths when food package was heated in the middle of each cavity. It is observed that with a lower cavity depth, return loss reduced. For example, when the cavity depth was 100 mm the reflected power at 915 MHz frequency was 3.67 dB that is 44 % of the incident power. As the cavity depth increased to 200 mm, reflection increased to 73% of the incident power.

Table 1: *A comparison of simulated and measured S_{11}-parameter (Return Loss)*

Frequency 915 MHz Cavity depth 100 mm	Simulated result in dB	Experimental result in dB
Return Loss	3.67	3.39

Figure 10(c) exhibits return loss behavior when food package was immersed within water and heated in the middle of the cavity. The presence of water resulted in more return loss, nearly 70% of the incident power at 915 MHz frequency. Figure 10(d) shows the return loss behavior when the dielectric properties of food changed as the temperature of the food increased. The values of complex permittivity of food at 50^0C, 80^0C, and 110^0C are 47 - j38.5, 45.3 - j48.6, and 42.6 - j60.7, respectively. Change in dielectric properties of food affected very little the return loss value. The return loss was measured at a cavity depth of 100 mm with no water around the food package at 915 MHz. The results are shown in Table 1.

Conclusions

It is shown that the FDTD modeling captures the overall behavior of a rectangular waveguide terminated into an oversize waveguide/cavity box to predict the mode behavior in empty cavity box throughout the volume space. Power deposition profile over surface/horizontal area of the food package as well as return loss parameter was described using a small but practical food processing applicator. The simulation results presented in this paper were verified by experiments. The following conclusions or general remarks can be drawn from this study:

- The main problem with single mode type applicator is its limitation in terms of geometrical dimensions. By choosing proper dimensions of oversize waveguide/ cavity box we can use this type of applicator as a single mode applicator with a better/ larger delimitation of the volume of heating material. Based on simulation, one can tailor the dimension of cavity box for required energy/mode distribution through out the space of the cavity box. Also, by changing the dimensions of the cavity box in x- and y-directions we can either spread the energy distribution or focus the energy distribution.
- It is observed that the power deposition profile over the food surface is very uneven when food is heated in open air, whereas it is approaching to be even when immersed in the water.
- The major drawback of this type applicator is a large return loss, which seems to be unavoidable. By using proper impedance matching device we can achieve better return loss. Also, by using Brewster angle approach, we can avoid reflections. The detailed understanding and design of the applicator need a comprehensive attention.

Acknowledgements

The authors would like to acknowledge the financial support of the Department of Defense Dual Use Science and Technology Program, U.S. Army Natick Soldier Center and Washington State University Agricultural Research Center that made this research possible.

References

Celuch, M. and Gwarek, W.K. 2000. Advanced features of FDTD modeling for microwave power applications, Presented at the 35th Microwave Power Symposium, Montreal, Canada, 2000.

Decareau, Robert V. 1985. Microwaves in the Food Processing Industry, Academic Press, New York.

Dibben D. and Metaxas, A.C. 1997. Frequency domain versus time domain finite element methods for calculation of fields in multimode cavities, IEEE Trans. Magnetics, MAG-32(2): 1468-1471.

Guy, A.W. 1971. Analyses of electromagnetic fields induced in biological tissues by thermographic studies on equivalent phantom models, IEEE Trans. Microwave Theory and Techniques, MTT-19: 205-214.

Guy, A.W., Lehmann, M.F., Stonebridge, J.B., and Sorensen, C.C. 1978. Development of a 915 MHz direct-contact applicator for therapeutic heating of tissues, IEEE Trans. Microwave Theory and Techniques, MTT-26(8): 550-563.

Kantoor, G. and Cetas, T.C. 1977. A comparative heating pattern study of direct contact applicators in microwave diathermy, Radio Science, Vol. 12: 111-120.

Kantoor, G. 1981. Evaluation and survey of microwave and radio-frequency applicators, Journal of Microwave Power, Vol.16:135-150.

Lau, R.W.M, Sheppard, R.J., Howard, G. and Bleehen, N.M. 1986. The modeling of biological systems in three dimensions using the tine domain finite-difference method:II. The application and experimental evaluation of the method in hyperthermia applicator design, Physics in Medicine and Biology, Vol.31: 1257-1267.

Marcysiak, M.C. and Gwarek, W.K. 1994. Higher-order modeling of media interfaces for enhanced FDTD analysis of microwave circuits, Proc. 24th European Microwave Conf., Cannes, Sept. 1994: 1530-1533.

Marcysiak, M.C. 1996. Time-domain approach to microwave circuit modeling : a view of general relations between TLM and FDTD, invited paper, Int. Journal of Microwaves and Millimeter-Wave Computer Aided Engineering, Vol.6(1): 36-46.

Marcysiak, M.C., Gwarek, W.K. and Sypniewski. 1998. A simple and effective approach to FD-TD modeling of structures including lossy metals, Asia-Pacific Microwave Conference Proc., Yokohoma, pp.991-993.

Marcysiak, M.C. and Gwarek, W.K. 1999. On the nature of the solutions produced by finite difference schemes in time domain, invited paper, Intl. Journal of Numerical Modeling-Electronics Networks, Devices and Fields, Vol .12: 23-40.

Metaxas, A.C. and Meredith, R. 1983. Industrial Microwave Heating, Peter Peregrinus Ltd., London, England.

Metaxas, A.C. 1996. Foundation of Electroheat: A Unified Approach, John Willey & Sons, New York.

Mirotznik, M. 1998. Conformal EM analysis, IEEE Spectrum, Vol.25(4): 84-85.

Risman, P. O. 1998. A microwave oven model: examples of microwave heating computations, Microwave World, Vol.19(1): 20-23.

Roussy, G. and Pearce, J.A. 1995. Foundations and Industrial Applications of Microwaves and Radio Frequency Fields, John Willey & Sons, New York.

Turner, P.F. and Kumar, L. 1982. Computer solution for applicator heating patterns, National Cancer Institute monograph, Vol.61: 521-523.

Waterman, F.M. and Nerlinger, R.E. 1986. The effect of coupling materials on specific absorption rate distributions at 915 MHz, Medical Physics, Vol.13: 391-395.

Wang Yifen, Wig, Timothy D, Tang J, and Hallberg L M 2003. Dielectric properties of foods relevant to RF and microwave pasteurization and sterilization, Journal of Food Engineering, Vol.57: 257-268.

Yee, K.S. 1966. Numerical solution of initial boundary value problems involving Maxwell's equations in isotropic media, IEEE Trans. Antennas Propagation., Vol. AP-14: 302-307.